Magnetic Damping in Epitaxial Iron Alloyed with Vanadium and Aluminum

David A. Smith[1,*], Anish Rai,[2,3] Youngmin Lim,[1] Timothy Q. Hartnett,[4] Arjun Sapkota,[2,3] Abhishek Srivastava,[2,3] Claudia Mewes,[2,3] Zijian Jiang,[1] Michael Clavel,[5] Mantu K. Hudait,[5] Dwight D. Viehland,[6] Jean J. Heremans,[1] Prasanna V. Balachandran,[4,7] Tim Mewes,[2,3] and Satoru Emori[1,†]

[1]*Department of Physics, Virginia Tech, Blacksburg, Virginia 24061, USA*
[2]*Department of Physics and Astronomy, University of Alabama, Tuscaloosa, Alabama 35487, USA*
[3]*Center for Materials for Information Technology (MINT), University of Alabama, Tuscaloosa, Alabama 35487, USA*
[4]*Department of Material Science and Engineering, University of Virginia, Charlottesville, Virginia 22904, USA*
[5]*Department of Electrical and Computer Engineering, Virginia Tech, Blacksburg, Virginia 24061, USA*
[6]*Department of Materials Science and Engineering, Virginia Tech, Blacksburg, Virginia 24061, USA*
[7]*Department of Mechanical and Aerospace Engineering, University of Virginia, Charlottesville, Virginia 22904, USA*

To develop low-moment, low-damping metallic ferromagnets for power-efficient spintronic devices, it is crucial to understand how magnetic relaxation is impacted by the addition of nonmagnetic elements. Here, we compare magnetic relaxation in epitaxial Fe films alloyed with light, nonmagnetic elements of V and Al. Fe-V alloys exhibit lower intrinsic damping compared with that of pure Fe, reduced by nearly a factor of 2, whereas damping in Fe-Al alloys increases with Al content. Our experimental and computational results indicate that reducing the density of states at the Fermi level, rather than the average atomic number, has a more significant impact on lowering damping in Fe alloyed with light elements. Moreover, Fe-V is confirmed to exhibit an intrinsic Gilbert damping parameter of about 0.001, which is among the lowest ever reported for ferromagnetic metals.

I. INTRODUCTION

The relaxation of magnetization dynamics (e.g., via Gilbert damping) plays important roles in many spintronic applications, including those based on magnetic switching [1,2], domain-wall motion [3,4], spin-wave propagation [5,6], and superfluidlike spin transport [7,8]. For devices driven by spin-torque precessional dynamics [1,9,10], the critical current density for switching is predicted to scale with the product of the Gilbert damping parameter and the saturation magnetization [2,11]. Thus, it is desirable to engineer magnetic materials that possess both low damping and low moment for energy-efficient operation. While some electrically insulating magnetic oxides have been considered for certain applications [5,12,13], it is essential to engineer low-damping, low-moment *metallic* ferromagnets for robust electrical readout via giant magnetoresistance and tunnel magnetoresistance. Fe is the elemental ferromagnet with the lowest intrinsic Gilbert

damping parameter ($\sim$0.002) [14,15], albeit with the highest saturation magnetization ($\sim$2.0 T). Recent experiments have reported that Gilbert damping can be further reduced by alloying Fe with Co (also a ferromagnetic element), with $Fe_{75}Co_{25}$ yielding an ultralow intrinsic Gilbert damping parameter of about 0.001 [16,17]. However, $Fe_{75}Co_{25}$ is close to the top of the Slater-Pauling curve, such that its saturation magnetization is greater than that of Fe by approximately 20% [18]. There is thus an unmet need to engineer ferromagnetic alloys that simultaneously exhibit lower damping and lower moment than those of Fe.

A promising approach towards low-damping, low-moment ferromagnetic metals is to introduce *nonmagnetic* elements into Fe. In addition to diluting the magnetic moment, nonmagnetic elements introduced into Fe can influence the spin-orbit coupling strength, ξ, which underlies spin relaxation via orbital and electronic degrees of freedom [19–21]. Simple atomic physics suggests that ξ is related to the average atomic number $\langle Z \rangle$ of the alloy, so that, conceivably, damping might be lowered by alloying Fe with lighter (lower-Z) elements. Indeed, motivated by the premise of lowering damping through

*smithd22@vt.edu
†semori@vt.edu

a reduced $\langle Z \rangle$, and presumably ξ, prior experiments have explored Fe thin films alloyed with V [20,22,23], Si [24], and Al [25]. However, the experimentally reported damping parameters for these alloys are often a factor of >2 higher [22,23,25] than that of the theoretically predicted intrinsic Gilbert damping parameter of about 0.002 in Fe [26] and do not exhibit a significant dependence on the alloy composition [20,23,24]. A possible issue is that the reported damping parameters, which are obtained from the frequency dependence of ferromagnetic resonance (FMR) linewidth with the film magnetized in plane, may include contributions from non-Gilbert relaxation induced by inhomogeneity and defects (e.g., two-magnon scattering) [27–36], which can be affected by alloying. Therefore, how Gilbert damping in Fe is impacted by alloying with low-Z elements remains an open question.

Here, we investigate the compositional dependence of magnetic relaxation at room temperature in epitaxial thin films of ferromagnetic Fe-V and Fe-Al alloys. Both alloys are crystalline bcc solid solutions and hence constitute excellent model systems. We employ two configurations of FMR measurements to gain complementary insights: (1) FMR with samples magnetized in the film plane (similar to prior experiments) to derive the "effective" Gilbert damping parameter, $\alpha_{\mathrm{eff}}^{\mathrm{IP}}$, which is found to include extrinsic magnetic relaxation due to two-magnon scattering, and (2) FMR with samples magnetized perpendicular to the film plane to quantify the intrinsic Gilbert damping parameter, α_{int}, which is free of the two-magnon scattering contribution.

Since Al ($Z = 13$) is a much lighter element than that of V ($Z = 23$), we might expect lower magnetic relaxation in Fe-Al than that in Fe-V, if the smaller $\langle Z \rangle$ lowers the intrinsic Gilbert damping via reduced ξ. Instead, we find a significant decrease in magnetic relaxation by alloying Fe with V, i.e., yielding an intrinsic Gilbert damping parameter of about 0.001, which is on par with the lowest values reported for ferromagnetic metals, whereas damping in Fe-Al alloys increases with Al content. These experimental results, combined with density-functional-theory calculations, point to the density of states at the Fermi level, $D(E_F)$, as a plausible dominant factor for the lower (higher) Gilbert damping in Fe-V (Fe-Al). We thus find that incorporating a low-Z element does not generally lower damping and that, rather, reducing $D(E_F)$ is an effective route for lower damping in Fe alloyed with a nonmagnetic element. Our findings confirm that Fe-V is an intrinsically ultralow-damping alloy, as theoretically predicted by Mankovsky *et al.* [26], which also possesses a lower saturation magnetization than those of Fe and Fe-Co. The combination of low damping and low moment makes Fe-V a highly promising material for practical metal-based spintronic applications.

II. FILM DEPOSITION AND STRUCTURAL PROPERTIES

Epitaxial $Fe_{100-x}V_x$ and $Fe_{100-x}Al_x$ thin films are grown using dc magnetron sputtering on (001)-oriented MgO substrates. Prior to deposition, the substrates are annealed at 600 °C for 2 h [37]. The base pressure prior to deposition is $<5 \times 10^{-8}$ Torr, and all films are grown with an Ar pressure of 3 mTorr. Fe and V (Al) 2" targets are dc cosputtered to deposit $Fe_{100-x}V_x$ ($Fe_{100-x}Al_x$) films at a substrate temperature of 200 °C. By adjusting the deposition power, we tune the deposition rate of each material (calibrated by x-ray reflectivity) to achieve the desired atomic percentage, x, of V (Al). All Fe-V and Fe-Al films have a thickness of 25 nm, which is well above the thickness regime where interfacial effects dominate [31,38]. The Fe-V (Fe-Al) films are capped with 3-nm-thick V (Al) deposited at room temperature to protect against oxidation, yielding a film structure of $MgO/Fe_{100-x}V_x(25\ nm)/V(3\ nm)$ or $MgO/Fe_{100-x}Al_x(25\ nm)/Al(3\ nm)$.

We confirm the epitaxial bcc structure of our thin films using high-resolution x-ray diffraction. The 2θ-ω scans show only the (002) peak of the film and the (002) and (004) peaks of the substrate, as shown in Fig. 1. Rocking curve scans of the film peaks show similar full width at half maximum values of about $1.3°$, irrespective of composition. The epitaxial relation between bcc Fe and MgO is well known [16,39]: the bcc film crystal is rotated $45°$ with respect to the substrate crystal, such that the [100] axis of the film lies parallel to the [110] axis of the substrate. The absence of the (001) film peak indicates that our epitaxial Fe-V and Fe-Al films are solid solutions rather than B2-ordered compounds [40].

III. MAGNETIC RELAXATION

A. In-plane ferromagnetic resonance

Many spintronic devices driven by precessional magnetization dynamics are based on in-plane-magnetized thin films. The equilibrium magnetization also lies in plane for soft ferromagnetic thin films dominated by shape anisotropy (i.e., negligible perpendicular magnetic anisotropy), as is the case for our epitaxial Fe-V and Fe-Al films. We therefore first discuss FMR results with films magnetized in plane. The in-plane FMR results further provide a basis for comparison with previous studies [20,22,23,25].

Samples are placed with the film side facing a coplanar waveguide (maximum frequency 50 GHz) and magnetized by an external field H (from a conventional electromagnet, maximum field 1.1 T) along the in-plane [100] and [110] axes of the films. Here, unless otherwise stated, we show results for $H \parallel$ [110] of the film. FMR spectra are acquired via field modulation by sweeping H and fixing the microwave excitation frequency.
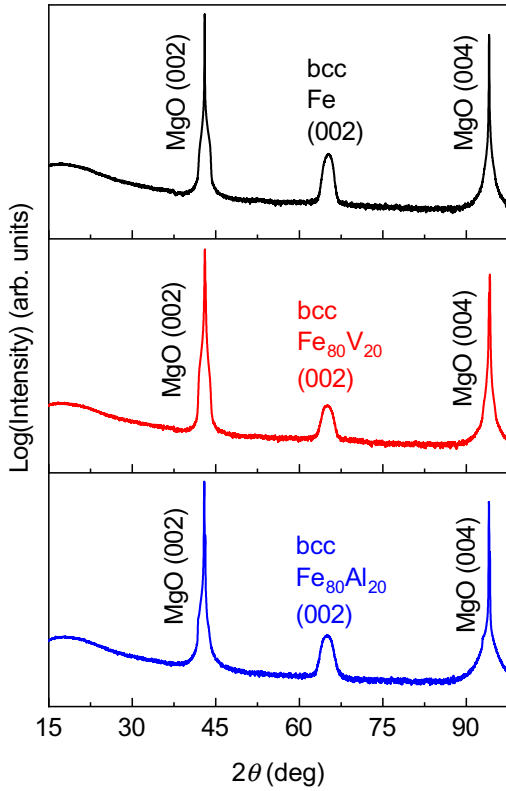
FIG. 1. (a) 2θ-ω x-ray diffraction scans showing (002) and (004) substrate and (002) film peaks for bcc Fe, $Fe_{80}V_{20}$, and $Fe_{80}Al_{20}$.
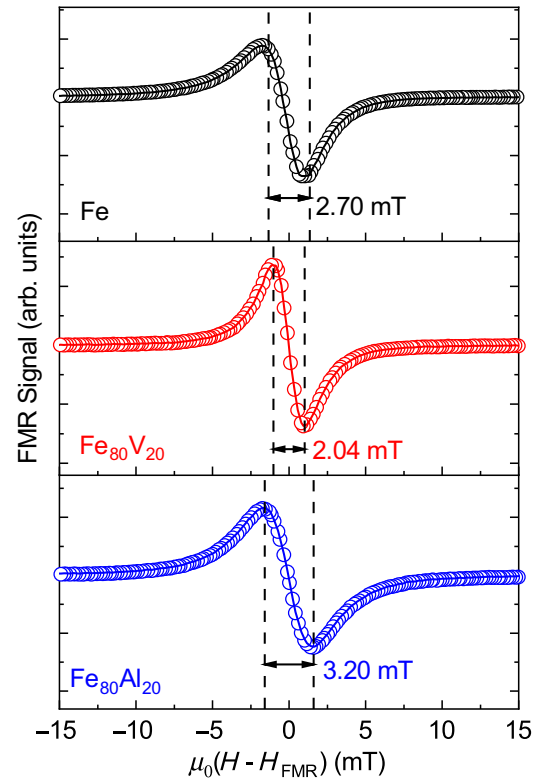

FIG. 2. FMR spectra at $f = 20$ GHz with the magnetic field, H, applied in the film plane and fitted using a Lorentzian derivative (solid curve) for Fe, $Fe_{80}V_{20}$, and $Fe_{80}Al_{20}$.

Exemplary spectra for Fe, $Fe_{80}V_{20}$, and $Fe_{80}Al_{20}$ are shown in Fig. 2, where we compare the peak-to-peak linewidths at a microwave excitation frequency of 20 GHz. We see that the linewidth for $Fe_{80}V_{20}$ shows about a 25% reduction compared with that of Fe. We further note that the linewidth for the $Fe_{80}V_{20}$ sample here is a factor of about 2 narrower than that in previously reported Fe-V [20]; a possible origin of the narrow linewidth is discussed later in Sec. III A. In contrast, $Fe_{80}Al_{20}$ shows an enhancement in linewidth over Fe, which is contrary to the expectation of lower magnetic relaxation with a lower average atomic number.

The FMR linewidth is generally governed not only by magnetic relaxation, but also by broadening contributions from magnetic inhomogeneities [28,41,42]. To disentangle the magnetic relaxation and inhomogeneous broadening contributions to the linewidth, the typical prescription is to fit the frequency, f, dependence of linewidth ΔH_{PP}^{IP} with the linear relation [41]

$$\Delta H_{PP}^{IP} = \Delta H_0^{IP} + \frac{h}{g\mu_B\mu_0}\frac{2}{\sqrt{3}}\alpha_{meas}^{IP}f, \qquad (1)$$

where h is the Planck constant, μ_B is the Bohr magneton, μ_0 is the permeability of free space, and g is the g factor obtained from the frequency dependence of the resonance field (see Sec. IV and the Supplemental Material [43,44]). In Eq. (1), the slope is attributed to viscous magnetic damping, which is captured by the measured damping parameter α_{meas}^{IP}, while the zero-frequency linewidth ΔH_0^{IP} is attributed to inhomogeneous broadening. Fitting with Eq. (1) is carried out for $f \geq 10$ GHz, where H is sufficiently large to saturate the films. As is evident from the results in Fig. 3, $Fe_{80}V_{20}$ has lower linewidths across all frequencies and a slightly lower slope, i.e., α_{meas}^{IP}. On the other hand, $Fe_{80}Al_{20}$ shows higher linewidths and a higher slope.

The measured viscous damping includes small contributions from eddy currents, parameterized by α_{eddy} (Supplemental Material [43,45]), and from radiative damping [46], given by α_{rad} (Supplemental Material [43]). Together, these contributions make up about 20% of the total α_{meas}^{IP} for pure Fe and decrease in magnitude with increasing V or Al content. We subtract these to obtain the effective in-plane Gilbert damping parameter

$$\alpha_{eff}^{IP} = \alpha_{meas}^{IP} - \alpha_{eddy} - \alpha_{rad}. \qquad (2)$$

As shown in Fig. 4(a), α_{eff}^{IP} remains either invariant or slightly decreases in $Fe_{100-x}V_x$ up to $x = 25$, whereas we observe a monotonic enhancement of α_{eff}^{IP} with Al content
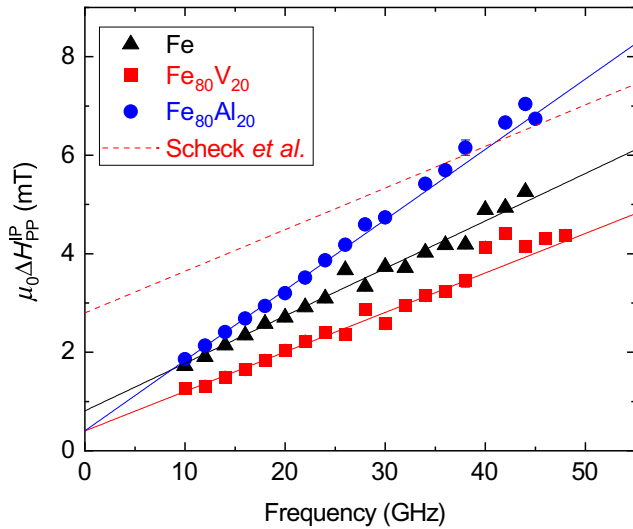
FIG. 3. FMR linewidths versus microwave frequency for the magnetic field applied within the plane of the film for three distinct alloys. Solid lines are linear fits, described by Eq. (1), from which the effective damping parameter and zero-frequency linewidth are determined. Dashed line represents the result for $Fe_{73}V_{27}$ from Scheck *et al.* [20].

in Fig. 4(b). These results point to lower (higher) damping in Fe-V (Fe-Al) and suggest a factor other than the average atomic number governing magnetic relaxation in these alloys. However, such a conclusion assumes that α_{eff}^{IP} is a reliable measure of intrinsic Gilbert damping. In reality, α_{eff}^{IP} may include a contribution from defect-induced two-magnon scattering [27–31,35,36], a well-known non-Gilbert relaxation mechanism in in-plane-magnetized epitaxial films [27,32–34,47]. We show in Sec. III B that substantial two-magnon scattering is indeed present in our Fe-V and Fe-Al alloy thin films.

Although Eq. (1) is not necessarily the correct framework for quantifying Gilbert damping in in-plane-magnetized thin films, we can gain an insight into the quality (homogeneity) of the films from ΔH_0^{IP}. For our samples, $\mu_0 \Delta H_0^{IP}$ is below about 1 mT [see Figs. 4(c) and 4(d)], which implies higher film quality for our Fe-V samples than that previously reported [20]. For example, $Fe_{73}V_{27}$ reported by Scheck *et al.* exhibits $\mu_0 \Delta H_0^{IP} \simeq$ 2.8 mT [20], whereas $Fe_{75}V_{25}$ in our study exhibits $\mu_0 \Delta H_0^{IP} \simeq 0.8$ mT. Although α_{eff}^{IP} is comparable between that reported by Scheck *et al.* and our study, the small ΔH_0^{IP} leads to overall much narrower linewidths in our Fe-V films (e.g., as shown in Figs. 2 and 3). We speculate that annealing of the MgO substrate prior to film deposition [37], a common practice for molecular beam epitaxy, facilitates high-quality epitaxial film growth and hence small ΔH_0^{IP}, even by sputtering.

B. Out-of-plane ferromagnetic resonance

To quantify intrinsic Gilbert damping, we perform broadband FMR with the film magnetized out of plane, which is the configuration that suppresses two-magnon scattering [28–31]. Samples are placed inside a W-band shorted-waveguide spectrometer (frequency range 70–110 GHz) in a superconducting electromagnet that enables measurements at fields of >4 T. This high-field range is well above the shape anisotropy field of ≤2 T for our films, and hence, sufficient to completely saturate the film out of plane.

The absence of two-magnon scattering in broadband out-of-plane FMR allows us to reliably obtain the measured viscous damping parameter, α_{meas}^{OP}, by fitting the linear frequency dependence of the linewidth ΔH_{PP}^{OP}, as

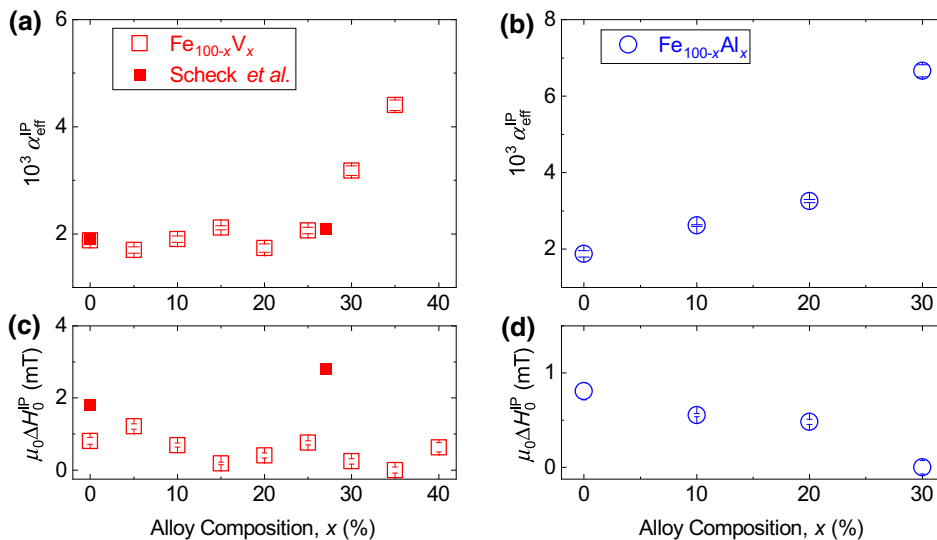FIG. 4. Effective damping parameter, α_{eff}^{IP}, for (a) $Fe_{100-x}V_x$ and (b) $Fe_{100-x}Al_x$, and zero-frequency linewidth, $\mu_0 \Delta H_0^{IP}$, for (c) $Fe_{100-x}V_x$ and (d) $Fe_{100-x}Al_x$, obtained from in-plane FMR. Solid symbols in (a) and (c) represent results reported by Scheck *et al.* [20].
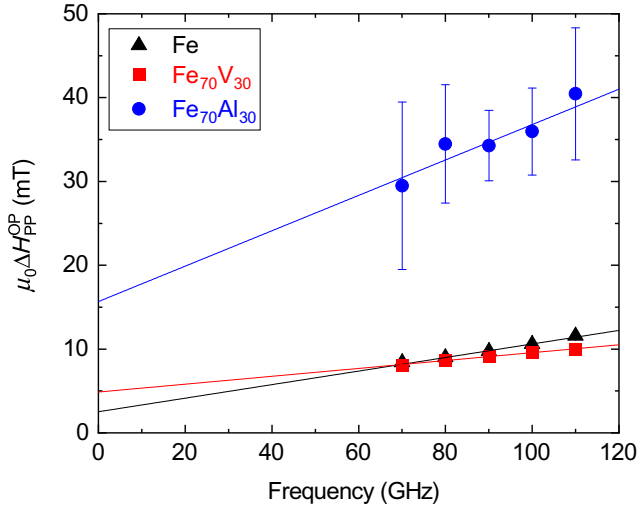
FIG. 5.   FMR linewidths versus applied microwave frequency for the magnetic field applied perpendicular to the plane of the film for three distinct alloys. Solid lines are linear fits, described by Eq. (3), from which the intrinsic Gilbert damping parameter and zero-frequency linewidth are determined.

shown in Fig. 5, with

$$\Delta H_{\mathrm{PP}}^{\mathrm{OP}} = \Delta H_0^{\mathrm{OP}} + \frac{h}{g\mu_B\mu_0}\frac{2}{\sqrt{3}}\alpha_{\mathrm{meas}}^{\mathrm{OP}}f. \qquad (3)$$

We note that the zero-frequency linewidth for the out-of-plane configuration ΔH_0^{OP} [Figs. 6(c) and 6(d)] is systematically greater than that for the in-plane configuration ΔH_0^{IP} [Figs. 4(c) and 4(d)]. Such a trend of $\Delta H_0^{\mathrm{OP}} > \Delta H_0^{\mathrm{IP}}$, often seen in epitaxial films [15,33,48], may be explained by the stronger contribution of inhomogeneity to the FMR field when the magnetic precessional orbit is circular, as is the case for out-of-plane FMR, compared with the case of the highly elliptical precession in in-plane FMR [41]; however, the detailed mechanisms contributing to the zero-frequency linewidth remain the subject of future work. The larger ΔH_0^{OP} at high V and Al concentrations may be due to broader distributions of anisotropy fields and saturation magnetization or the presence of a secondary crystal phase that is below the resolution of our x-ray diffraction results.

The absence of two-magnon scattering in out-of-plane FMR allows us to quantify the intrinsic Gilbert damping parameter

$$\alpha_{\mathrm{int}} = \alpha_{\mathrm{meas}}^{\mathrm{OP}} - \alpha_{\mathrm{eddy}}, \qquad (4)$$

by again subtracting the eddy current contribution α_{eddy}. Since we utilize a shorted waveguide, the contribution due to radiative damping does not apply.

From the compositional dependence of α_{int}, as summarized in Fig. 6(a) [49], a reduction in intrinsic Gilbert

damping is evidenced with V alloying. Our observation is in contrast to previous experiments on Fe-V alloys [20,22,23], where the reported damping parameters remain >0.002 and depend weakly on the V concentration. In particular, the observed minimum of $\alpha_{\mathrm{int}} \sim 0.001$ at $x \sim 25 - 30$ is approximately half of the lowest Gilbert damping parameter previously reported for Fe-V [20] and that of pure Fe [15]. The low α_{int} here is also comparable to the lowest damping parameters reported for ferromagnetic metals, such as $Fe_{75}Co_{25}$ [16,17] and Heusler compounds [50–52]. Moreover, the reduced intrinsic damping by alloying Fe with V is qualitatively consistent with the computational prediction by Mankovsky *et al.* [26], as shown by the curve in Fig. 6(a). Our experimental finding therefore confirms that Fe-V is indeed an intrinsically ultralow-damping ferromagnet that possesses a smaller saturation magnetization than that of Fe.

In contrast to the reduction of α_{int} observed in Fe-V alloys, Fe-Al shows an increase in intrinsic damping with increasing Al concentration, as seen in Fig. 6(b). Recalling that Al has an atomic number of $Z = 13$, which is lower than that of $Z = 23$ for V, this trend clashes with the expectation that lower $\langle Z \rangle$ reduces the intrinsic Gilbert damping through a reduction of the atomic spin-orbit coupling. Thus, we are required to consider an alternative mechanism to explain the higher (lower) damping in Fe-Al (Fe-V), which we discuss further in Sec. V.

C. Magnetic relaxation: Practical considerations

For both Fe-V and Fe-Al alloys, α_{int} derived from out-of-plane FMR [Figs. 6(a) and 6(b)] is consistently lower than that of $\alpha_{\mathrm{eff}}^{\mathrm{IP}}$ derived from in-plane FMR [Figs. 4(a) and 4(b)]. This discrepancy between α_{int} and $\alpha_{\mathrm{eff}}^{\mathrm{IP}}$ implies a two-magnon scattering contribution to magnetic relaxation in the in-plane configuration [Figs. 4(a) and 4(b)]. For many applications, including spin-torque oscillators and magnonic devices, it is crucial to minimize magnetic relaxation in in-plane-magnetized thin films. While the in-plane magnetic relaxation ($\alpha_{\mathrm{eff}}^{\mathrm{IP}} \simeq 0.002$) is already quite low for the Fe-V alloys shown here, the low intrinsic Gilbert damping ($\alpha_{\mathrm{int}} \simeq 0.001$) points to the possibility of even lower relaxation and narrower FMR linewidths by minimizing two-magnon scattering and inhomogeneous linewidth broadening. Such ultralow magnetic relaxation in Fe-V alloy thin films may be achieved by optimizing structural properties through growth conditions [16] or seed-layer engineering [53].

While ultralow intrinsic Gilbert damping values are confirmed in high-quality epitaxial Fe-V, it would be desirable for device integration to understand how magnetic relaxation in Fe-V would be impacted by the presence of grain boundaries, i.e., in polycrystalline thin films. Reports on polycrystalline Fe-Co [17,53] suggest intrinsic damping
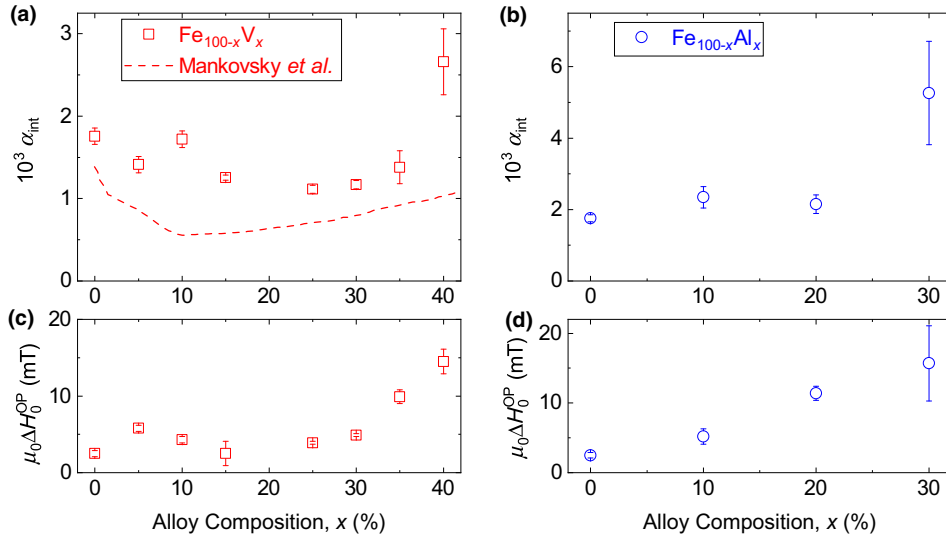
FIG. 6. Intrinsic Gilbert damping parameter, α_{int}, for (a) $Fe_{100-x}V_x$ and (b) $Fe_{100-x}Al_x$, and zero-frequency linewidth, $\mu_0 \Delta H_0^{\mathrm{OP}}$, for (c) $Fe_{100-x}V_x$ and (d) $Fe_{100-x}Al_x$, obtained from out-of-plane FMR. In (a), dashed curve shows the predicted intrinsic damping parameter computed by Mankovsky *et al.* [26].

values comparable to those seen in epitaxial Fe-Co [16]. While beyond the scope of this study, our future work will explore the possibility of low damping in polycrystalline Fe-V thin films.

IV. SPECTROSCOPIC PARAMETERS

The results presented so far reveal that magnetic relaxation is reduced by alloying Fe with V, whereas it is increased by alloying Fe with Al. On the other hand, Fe-V and Fe-Al alloys exhibit similar compositional dependence of the spectroscopic parameters: effective magnetization, M_{eff} (here, equivalent to saturation magnetization, M_s); magnetocrystalline anisotropy field, H_k; and the g factor, g, all of which are quantified by fitting the frequency dependence of resonance field (see the Supplemental Material [43]). As shown in Fig. 7(a), there is a systematic reduction in M_{eff} with increasing concentration of V and Al. We also note in Fig. 7(b) a gradual reduction in magnitude of the in-plane cubic anisotropy. Both of these trends are expected, as magnetic Fe atoms are replaced with nonmagnetic atoms of V and Al. The reduction of M_{eff} by about 20% in the ultralow-damping $Fe_{100-x}V_x$ alloys with $x = 25 - 30$, compared with that of pure Fe, is of particular practical interest. The saturation magnetization of these Fe-V alloys is on par with commonly used soft ferromagnetic alloys (e.g., $Ni_{80}Fe_{20}$ [54], (Co, Fe)B [55]), but the damping parameter of Fe-V is several times lower. Further, while Fe-V and Fe-Co in the optimal composition window show similarly low intrinsic damping parameters, Fe-V provides the advantage of a lower moment. With the product $\alpha_{\mathrm{int}} M_{\mathrm{eff}}$ approximately proportional to the critical current density to excite precessional dynamics by spin torque [2,11], Fe-V is expected to be a superior material platform for low-power spintronic devices.

The g factor $g = 2(1 + \mu_L / \mu_S)$ is related to the orbital moment μ_L and spin moment μ_S; the deviation from the spin-only value of $g = 2.00$ provides an insight into the strength of spin-orbit coupling, ξ [56]. As seen in Fig. 7(c), g increases by 1–2% with both V and Al alloying, which suggests that ξ increases slightly with the addition of these low-Z elements. This finding verifies that $\langle Z \rangle$ is not
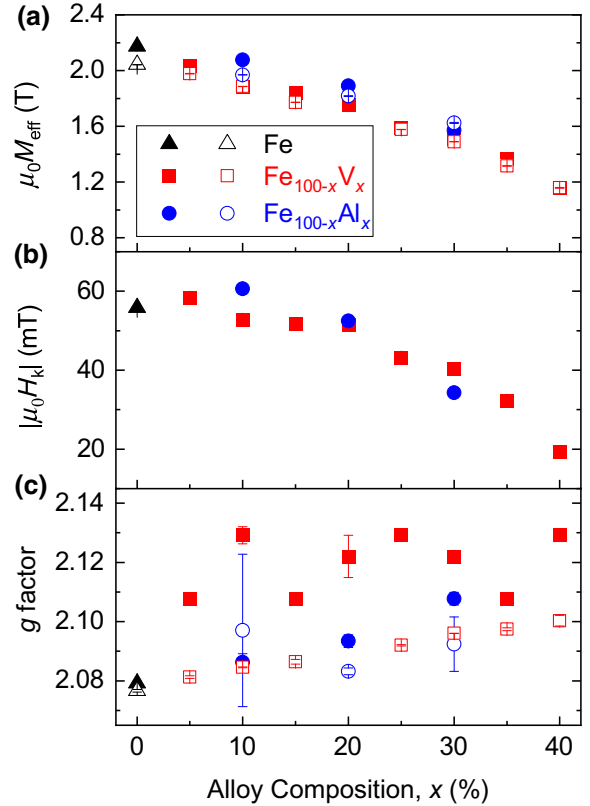

FIG. 7. (a) Effective magnetization, (b) in-plane cubic anisotropy field, and (c) g factor versus V and Al concentration. Solid (open) markers represent data from in-plane (out-of-plane) measurements.
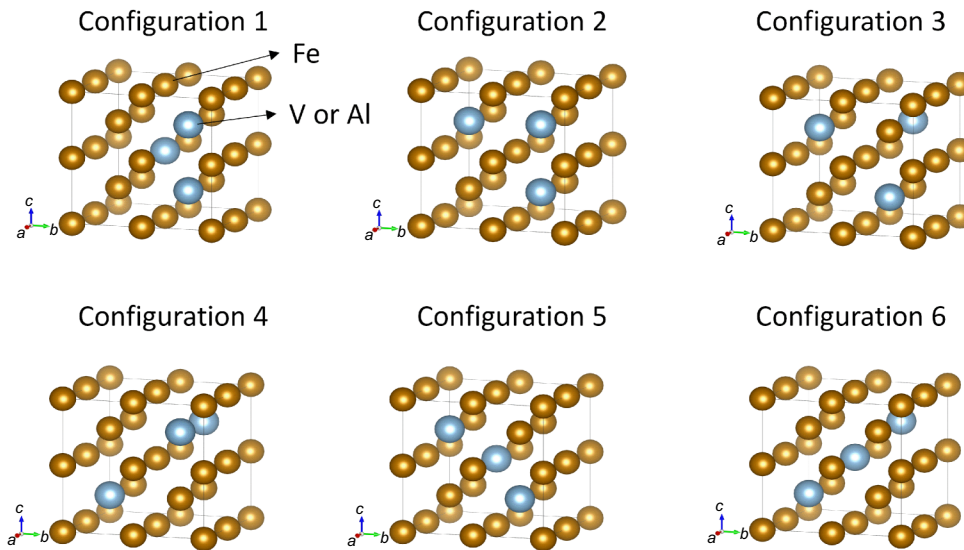
FIG. 8. Six unique atomic configurations from the super-cell program for mimicking $Fe_{81.25}V_{18.75}$ or $Fe_{81.25}Al_{18.75}$ solid solutions.

necessarily a good predictor of ξ in a solid. Moreover, the higher g for Fe-V is inconsistent with the scenario for lower damping linked to a reduced spin-orbit coupling. Thus, spin-orbit coupling alone cannot explain the observed behavior of Gilbert damping in Fe alloyed with low-Z elements.

V. DISCUSSION

In contrast to what has been suggested by prior experimental studies [20,22–25], we show that the reduction of average atomic number by alloying with a light element (e.g., Al in this case) does not generally lower the intrinsic Gilbert damping of Fe. A possible source for the qualitatively distinct dependencies of damping on V and Al contents is the density of states at the Fermi level, $D(E_F)$: it is predicted theoretically that the intrinsic Gilbert damping parameter is reduced with decreasing $D(E_F)$, since $D(E_F)$ governs the availability of states for spin-polarized electrons to scatter into [21,26,57–59]. Such a correlation between lower damping and smaller $D(E_F)$ has been reported by recent experiments on Fe-Co alloys [17,54], Fe-Rh alloys [40], Co-Ni alloys [60], and Heusler compounds [50,52,61]. The similarity in the predicted composition dependence of the Gilbert damping parameter for Fe-Co and Fe-V [26] suggests that the low damping of Fe-V may be correlated with reduced $D(E_F)$. However, no prior experiment has corroborated this correlation for Fe-V or other alloys of Fe and light elements.

We therefore examine whether the lower (higher) damping in Fe-V (Fe-Al) compared with that of Fe can be qualitatively explained by $D(E_F)$. Utilizing the Quantum ESPRESSO [62] package to perform density-functional-theory calculations (details are given in the Supplemental Material [43,63–67]), we calculate the density of states for Fe, $Fe_{81.25}V_{18.75}$, and $Fe_{81.25}Al_{18.75}$. It should be recalled

that, although Fe-V and Fe-Al films measured experimentally here are single crystalline, they are solid solutions in which V or Al atoms replace Fe atoms at arbitrary bcc lattice sites. Therefore, for each of the binary alloys, we compute six distinct atomic configurations in a $2 \times 2 \times 2$ supercell, as shown in Fig. 8. The spin-split density of states for each unique atomic configuration is indicated by a curve in Fig. 9. Here, $D(E_F)$ is the sum of the states for the spin-up and spin-down bands, averaged over results from the six distinct atomic configurations.

As summarized in Fig. 9 and Table I, Fe-V has a smaller $D(E_F)$ than that of Fe, whereas Fe-Al has a larger $D(E_F)$. These calculation results confirm a smaller (larger) availability of states for spin-polarized electrons to scatter into in Fe-V (Fe-Al), qualitatively consistent with the lower (higher) intrinsic Gilbert damping in Fe-V (Fe-Al).

We remark that this correlation between damping and $D(E_F)$ is known to hold particularly well in the limit of low electronic scattering rates, τ^{-1}, where intraband scattering dominates [21,58]. Gilmore *et al.* [21] have pointed out that, at sufficiently high electronic scattering rates, i.e., when $\hbar\tau^{-1}$ is large enough that interband scattering is substantial, the simple correlation between the strength of Gilbert damping and $D(E_F)$ breaks down. It is unclear whether our Fe-V and Fe-Al alloy films at room temperature are in the intraband- or interband-dominated regime. Schoen *et al.* have argued that polycrystalline Fe-Co alloy films, with a higher degree of structural disorder and likely higher electronic scattering rates than those of our epitaxial films, at room temperature are still well within the intraband-dominated regime [17]. On the other hand, a recent temperature-dependent study on epitaxial Fe suggests the coexistence of intraband and interband contributions at room temperature [15]. A consistent explanation for the observed room-temperature intrinsic damping in our alloy films is that the
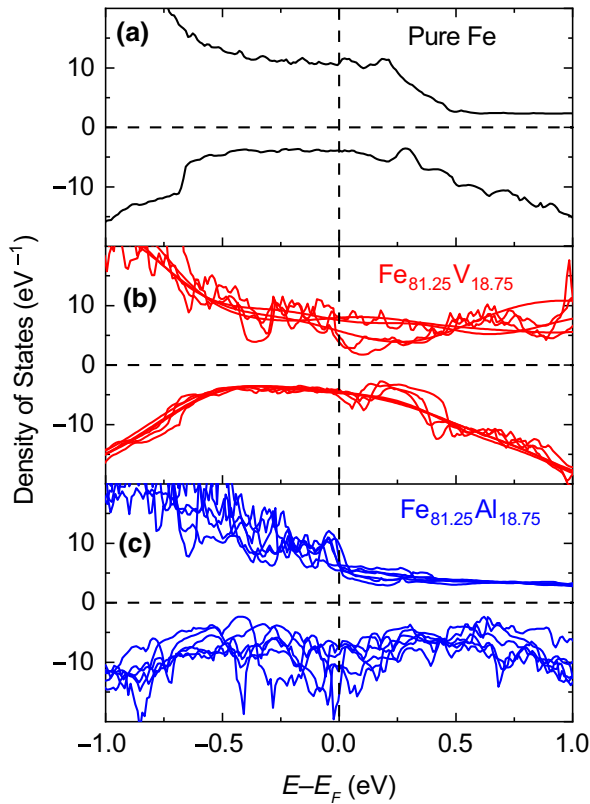
FIG. 9. Calculated spin-up (positive) and spin-down (negative) densities of states for (a) Fe, (b) $Fe_{81.25}V_{18.75}$, and (c) $Fe_{81.25}Al_{18.75}$. Results from the six distinct atomic configurations are shown in (b),(c); average densities of states at E_F for $Fe_{81.25}V_{18.75}$ and $Fe_{81.25}Al_{18.75}$ are shown in Table I.

interband contribution depends weakly on alloy composition; it appears reasonable to conclude that $D(E_F)$, primarily through the intraband contribution, governs the difference in intrinsic Gilbert damping among Fe, Fe-V, and Fe-Al.

VI. SUMMARY

We experimentally investigate magnetic relaxation in epitaxial thin films of Fe alloyed with low-atomic-number

TABLE I. Number of spin-up and spin-down states at E_F. For $Fe_{81.25}V_{18.75}$ and $Fe_{81.25}Al_{18.75}$, the average and standard deviation of values for the six distinct atomic configurations (cf. Fig. 8) are shown.

	Number of spin-up states (eV^{-1}) at E_F	Number of spin-down states (eV^{-1}) at E_F
Fe	10.90	3.44
$Fe_{81.25}V_{18.75}$	6.28 ± 1.80	4.61 ± 0.43
$Fe_{81.25}Al_{18.75}$	6.81 ± 1.58	10.20 ± 3.03

nonmagnetic elements V and Al. We observe a reduction in the intrinsic Gilbert damping parameter to $\alpha_{int} \sim 0.001$ in Fe-V films, comparable to the lowest-damping ferromagnetic metals reported to date. In contrast, an increase in damping is observed with the addition of Al, demonstrating that a smaller average atomic number does not necessarily lower intrinsic damping in an alloy. Furthermore, our results on Fe-V and Fe-Al cannot be explained by the change in spin-orbit coupling through alloying. Instead, we conclude that the density of states at the Fermi level plays a larger role in determining the magnitude of damping in Fe alloyed with lighter elements. Our work also confirms Fe-V alloys as promising ultralow-damping, low-moment metallic materials for practical power-efficient spin-torque devices.

Data that support the findings of this study are available from the corresponding author upon reasonable request.

[1] A. Brataas, A. D. Kent, and H. Ohno, Current-induced torques in magnetic materials, Nat. Mater. **11**, 372 (2012).

[2] J. Z. Sun, Spin-current interaction with a monodomain magnetic body: A model study, Phys. Rev. B **62**, 570 (2000).

[3] T. Weindler, H. G. Bauer, R. Islinger, B. Boehm, J. Y. Chauleau, and C. H. Back, Magnetic Damping: Domain Wall Dynamics Versus Local Ferromagnetic Resonance, Phys. Rev. Lett. **113**, 237204 (2014).

[4] A. Mougin, M. Cormier, J. P. Adam, P. J. Metaxas, and J. Ferré, Domain wall mobility, stability and Walker breakdown in magnetic nanowires, Europhys. Lett. **78**, 57007 (2007).

[5] A. V. Chumak, V. I. Vasyuchka, A. A. Serga, and B. Hillebrands, Magnon spintronics, Nat. Phys. **11**, 453 (2015).

[6] J. Han, P. Zhang, J. T. Hou, S. A. Siddiqui, and L. Liu, Mutual control of coherent spin waves and magnetic domain walls in a magnonic device, Science **366,** 1121 (2019).

[7] E. B. Sonin, Spin currents and spin superfluidity, Adv. Phys. **59,** 181 (2010).

[8] Y. Tserkovnyak, Perspective: (Beyond) spin transport in insulators, J. Appl. Phys. **124,** 190901 (2018).

[9] D. C. Ralph and M. D. Stiles, Spin transfer torques, J. Magn. Magn. Mater. **320,** 1190 (2008).

[10] A. Manchon, J. Železný, I. M. Miron, T. Jungwirth, J. Sinova, A. Thiaville, K. Garello, and P. Gambardella, Current-induced spin-orbit torques in ferromagnetic and antiferromagnetic systems, Rev. Mod. Phys. **91,** 035004 (2019).

[11] J. C. Slonczewski, Currents and torques in metallic magnetic multilayers, J. Magn. Magn. Mater. **247,** 324 (2002).

[12] S. Emori, D. Yi, S. Crossley, J. J. Wisser, P. P. Balakrishnan, B. Khodadadi, P. Shafer, C. Klewe, A. T. N'diaye, B. T. Urwin, K. Mahalingam, B. M. Howe, H. Y. Hwang, E. Arenholz, and Y. Suzuki, Ultralow damping in nanometer-thick epitaxial spinel ferrite thin films, Nano Lett. **18,** 4273 (2018).

[13] L. J. Cornelissen, J. Liu, R. A. Duine, J. Ben Youssef, and B. J. Van Wees, Long-distance transport of magnon spin information in a magnetic insulator at room temperature, Nat. Phys. **11,** 1022 (2015).

[14] M. Oogane, T. Wakitani, S. Yakata, R. Yilgin, Y. Ando, A. Sakuma, and T. Miyazaki, Magnetic damping in ferromagnetic thin films, Jpn. J. Appl. Phys. **45,** 3889 (2006).

[15] B. Khodadadi, A. Rai, A. Sapkota, A. Srivastava, B. Nepal, Y. Lim, D. A. Smith, C. Mewes, S. Budhathoki, A. J. Hauser, M. Gao, J.-F. Li, D. D. Viehland, Z. Jiang, J. J. Heremans, P. V. Balachandran, T. Mewes, and S. Emori, Conductivitylike Gilbert Damping due to Intraband Scattering in Epitaxial Iron, Phys. Rev. Lett. **124,** 157201 (2020).

[16] A. J. Lee, J. T. Brangham, Y. Cheng, S. P. White, W. T. Ruane, B. D. Esser, D. W. McComb, P. C. Hammel, and F. Yang, Metallic ferromagnetic films with magnetic damping under 1.4×10^{-3}, Nat. Commun. **8,** 1 (2017).

[17] M. A. W. Schoen, D. Thonig, M. L. Schneider, T. J. Silva, H. T. Nembach, O. Eriksson, O. Karis, and J. M. Shaw, Ultra-low magnetic damping of a metallic ferromagnet, Nat. Phys. **12,** 839 (2016).

[18] M. A. W. Schoen, J. Lucassen, H. T. Nembach, T. J. Silva, B. Koopmans, C. H. Back, and J. M. Shaw, Magnetic properties of ultrathin 3d transition-metal binary alloys. I. Spin and orbital moments, anisotropy, and confirmation of slater-pauling behavior, Phys. Rev. B **95,** 134410 (2017).

[19] P. He, X. Ma, J. W. Zhang, H. B. Zhao, G. Lüpke, Z. Shi, and S. M. Zhou, Quadratic Scaling of Intrinsic Gilbert Damping with Spin-Orbital Coupling in $L1_0$ FePdPt Films: Experiments and Ab Initio Calculations, Phys. Rev. Lett. **110,** 077203 (2013).

[20] C. Scheck, L. Cheng, I. Barsukov, Z. Frait, and W. E. Bailey, Low Relaxation Rate in Epitaxial Vanadium-Doped Ultrathin Iron Films, Phys. Rev. Lett. **98,** 117601 (2007).

[21] K. Gilmore, Y. U. Idzerda, and M. D. Stiles, Spin-orbit precession damping in transition metal ferromagnets (invited), J. Appl. Phys **103,** 07D303 (2008).

[22] J.-M. L. Beaujour, A. D. Kent, D. W. Abraham, and J. Z. Sun, Ferromagnetic resonance study of polycrystalline $Fe_{1-x}V_x$ alloy thin films, J. Appl. Phys. **103,** 07B519 (2008).

[23] T. Devolder, T. Tahmasebi, S. Eimer, T. Hauet, and S. Andrieu, Compositional dependence of the magnetic properties of epitaxial FeV/MgO thin films, Appl. Phys. Lett. **103,** 242410 (2013).

[24] I. Barsukov, S. Mankovsky, A. Rubacheva, R. Meckenstock, D. Spoddig, J. Lindner, N. Melnichak, B. Krumme, S. I. Makarov, H. Wende, H. Ebert, and M. Farle, Magnetocrystalline anisotropy and Gilbert damping in iron-rich $Fe_{1-x}Si_x$ thin films, Phys. Rev. B **84,** 180405(R) (2011).

[25] I. Kanada, A. Cruce, T. Mewes, S. Wu, C. Mewes, G. Mankey, and T. Suzuki, Soft magnetic properties and damping parameter of (FeCo)-Al alloy thin films, AIP Adv. **7,** 056105 (2017).

[26] S. Mankovsky, D. Ködderitzsch, G. Woltersdorf, and H. Ebert, First-principles calculation of the Gilbert damping parameter via the linear response formalism with application to magnetic transition metals and alloys, Phys. Rev. B **87,** 014430 (2013).

[27] R. D. McMichael, M. D. Stiles, P. J. Chen, and W. F. Egelhoff, Ferromagnetic resonance linewidth in thin films coupled to NiO, J. Appl. Phys. **83,** 7037 (1998).

[28] R. D. McMichael and P. Krivosik, Classical model of extrinsic ferromagnetic resonance linewidth in ultrathin films, IEEE Trans. Magn. **40,** 2 (2004).

[29] R. Arias and D. L. Mills, Extrinsic contributions to the ferromagnetic resonance response of ultrathin films, Phys. Rev. B **60,** 7395 (1999).

[30] G. Woltersdorf and B. Heinrich, Two-magnon scattering in a self-assembled nanoscale network of misfit dislocations, Phys. Rev. B **69,** 184417 (2004).

[31] K. Lenz, H. Wende, W. Kuch, K. Baberschke, K. Nagy, and A. Jánossy, Two-magnon scattering and viscous Gilbert damping in ultrathin ferromagnets, Phys. Rev. B **73,** 144424 (2006).

[32] K. Zakeri, J. Lindner, I. Barsukov, R. Meckenstock, M. Farle, U. Von Hörsten, H. Wende, W. Keune, J. Rocker, S. S. Kalarickal, K. Lenz, W. Kuch, K. Baberschke, and Z. Frait, Spin dynamics in ferromagnets: Gilbert damping and two-magnon scattering, Phys. Rev. B **76,** 104416 (2007).

[33] S. Emori, U. S. Alaan, M. T. Gray, V. Sluka, Y. Chen, A. D. Kent, and Y. Suzuki, Spin transport and dynamics in all-oxide perovskite $La_{2/3}Sr_{1/3}MnO_3/SrRuO_3$ bilayers probed by ferromagnetic resonance, Phys. Rev. B **94,** 224423 (2016).

[34] W. K. Peria, T. A. Peterson, A. P. Mcfadden, T. Qu, C. Liu, C. J. Palmstrøm, and P. A. Crowell, Interplay of large two-magnon ferromagnetic resonance linewidths and low Gilbert damping in Heusler thin films, Phys. Rev. B **101,** 134430 (2020).

[35] C. Mewes and T. Mewes, in *Handbook of Nanomagnetism: Applications and Tools* (Pan Stanford, Boca Raton, FL, 2015).

[36] J. Lindner, K. Lenz, E. Kosubek, K. Baberschke, D. Spoddig, R. Meckenstock, J. Pelzl, Z. Frait, and D. L. Mills, Non-Gilbert-type damping of the magnetic relaxation in ultrathin ferromagnets: Importance of magnon-magnon scattering, Phys. Rev. B **68**, 060102(R) (2003).

[37] M. Rickart, B. F. P. Roos, T. Mewes, J. Jorzick, S. O. Demokritov, and B. Hillebrands, Morphology of epitaxial metallic layers on MgO substrates: Influence of submonolayer carbon contamination, Surf. Sci. **495**, 68 (2001).

[38] L. Chen, S. Mankovsky, S. Wimmer, M. A. W. Schoen, H. S. Körner, M. Kronseder, D. Schuh, D. Bougeard, H. Ebert, D. Weiss, and C. H. Back, Emergence of anisotropic Gilbert damping in ultrathin Fe layers on GaAs(001), Nat. Phys. **14**, 490 (2018).

[39] C. Scheck, L. Cheng, and W. E. Bailey, Low damping in epitaxial sputtered iron films, Appl. Phys. Lett. **88**, 252510 (2006).

[40] T. Usami, M. Itoh, and T. Taniyama, Compositional dependence of Gilbert damping constant of epitaxial $Fe_{100-x}Rh_x$ thin films, Appl. Phys. Lett. **115**, 142403 (2019).

[41] B. Heinrich, *Ultrathin Magn. Struct. III* (Springer-Verlag, Berlin/Heidelberg, 2005), pp. 143–210.

[42] R. D. McMichael, A mean-field model of extrinsic line broadening in ferromagnetic resonance, J. Appl. Phys. **103**, 07B114 (2008).

[43] See the Supplemental Material at http://link.aps.org/supplemental/10.1103/PhysRevApplied.14.034042 for details regarding the fitting of FMR spectra, frequency dependence of the FMR resonance field, eddy current and radiative damping corrections, and details regarding the density of states calculations.

[44] M. Farle, Ferromagnetic resonance of ultrathin metallic layers, Rep. Prog. Phys. **61**, 755 (1998).

[45] J. M. Lock, Eddy current damping in metallic ferromagnetic films, Brit. J. Appl. Phys **17**, 1645 (1966).

[46] M. A. W. Schoen, J. M. Shaw, H. T. Nembach, M. Weiler, and T. J. Silva, Radiative damping in waveguide-based ferromagnetic resonance measured via analysis of perpendicular standing spin waves in sputtered permalloy films, Phys. Rev. B **92**, 184417 (2015).

[47] H. K. Lee, I. Barsukov, A. G. Swartz, B. Kim, L. Yang, H. Y. Hwang, and I. N. Krivorotov, Magnetic anisotropy, damping, and interfacial spin transport in Pt/LSMO bilayers, AIP Adv. **6**, 055212 (2016).

[48] H. Chang, P. Li, W. Zhang, T. Liu, A. Hoffmann, L. Deng, and M. Wu, Nanometer-thick yttrium iron garnet films with extremely low damping, IEEE Magn. Lett. **5**, 6700104 (2014).

[49] We are unable to carry out out-of-plane FMR measurements for Fe-V with $x = 20$ [Figs. 6(a) and 6(c)], as the sample had been severely damaged during transit.

[50] S. Mizukami, D. Watanabe, M. Oogane, Y. Ando, Y. Miura, M. Shirai, and T. Miyazaki, Low damping constant for Co_2FeAl heusler alloy films and its correlation with density of states, J. Appl. Phys. **105**, 07D306 (2009).

[51] P. Dürrenfeld, F. Gerhard, J. Chico, R. K. Dumas, M. Ranjbar, A. Bergman, L. Bergqvist, A. Delin, C. Gould, L. W. Molenkamp, and J. Akerman, Tunable damping, saturation magnetization, and exchange stiffness of half-Heusler NiMnSb thin films, Phys. Rev. B **92**, 214424 (2015).

[52] C. Guillemard, S. Petit-Watelot, L. Pasquier, D. Pierre, J. Ghanbaja, J.-C. Rojas-Sánchez, A. Bataille, J. Rault, P. Le Fèvre, F. Bertran, and S. Andrieu, Ultralow Magnetic Damping in Co_2Mn-Based Heusler Compounds: Promising Materials for Spintronics, Phys. Rev. Appl. **11**, 064009 (2019).

[53] E. R. J. Edwards, H. T. Nembach, and J. M. Shaw, $Co_{25}Fe_{75}$ Thin Films with Ultralow Total Damping of Ferromagnetic Resonance, Phys. Rev. Appl. **11**, 054036 (2019).

[54] M. A. W. Schoen, J. Lucassen, H. T. Nembach, B. Koopmans, T. J. Silva, C. H. Back, and J. M. Shaw, Magnetic properties in ultrathin 3d transition-metal binary alloys. II. Experimental verification of quantitative theories of damping and spin pumping, Phys. Rev. B **95**, 134411 (2017).

[55] A. Conca, J. Greser, T. Sebastian, S. Klingler, B. Obry, B. Leven, and B. Hillebrands, Low spin-wave damping in amorphous $Co_{40}Fe_{40}B_{20}$ thin films, J. Appl. Phys. **113**, 213909 (2013).

[56] J. M. Shaw, H. T. Nembach, T. J. Silva, and C. T. Boone, Precise determination of the spectroscopic g-factor by use of broadband ferromagnetic resonance spectroscopy, J. Appl. Phys. **114**, 243906 (2013).

[57] K. Gilmore, Y. U. Idzerda, and M. D. Stiles, Identification of the Dominant Precession-Damping Mechanism in Fe, Co, and Ni by First-Principles Calculations, Phys. Rev. Lett. **99**, 027204 (2007).

[58] H. Ebert, S. Mankovsky, D. Ködderitzsch, and P. J. Kelly, Ab Initio Calculation of the Gilbert Damping Parameter via the Linear Response Formalism, Phys. Rev. Lett. **107**, 066603 (2011).

[59] C. Liu, C. K. A. Mewes, M. Chshiev, T. Mewes, and W. H. Butler, Origin of low Gilbert damping in half metals, Appl. Phys. Lett. **95**, 022509 (2009).

[60] S. J. Xu, J. Y. Shi, Y. S. Hou, Z. Zheng, H. B. Zhao, R. Q. Wu, S. M. Zhou, Z. Shi, and W. J. Fan, Tuning of the intrinsic magnetic damping parameter in epitaxial CoNi(001) films: Role of the band-filling effect, Phys. Rev. B **100**, 024403 (2019).

[61] M. Oogane, T. Kubota, Y. Kota, S. Mizukami, H. Naganuma, A. Sakuma, and Y. Ando, Gilbert magnetic damping constant of epitaxially grown Co-based Heusler alloy thin films, Appl. Phys. Lett. **96**, 252501 (2010).

[62] P. Giannozzi, *et al.*, Quantum ESPRESSO: A modular and open-source software project for quantum simulations of materials, J. Phys. Condens. Matter **21**, 395502 (2009).

[63] J. P. Perdew, A. Ruzsinszky, G. I. Csonka, O. A. Vydrov, G. E. Scuseria, L. A. Constantin, X. Zhou, and K. Burke, Restoring the Density-Gradient Expansion for Exchange in Solids and Surfaces, Phys. Rev. Lett. **100**, 136406 (2008).

[64] D. Vanderbilt, Soft self-consistent pseudopotentials in a generalized eigenvalue formalism, Phys. Rev. B **41**, 7892 (1990).

[65] H. J. Monkhorst and J. D. Pack, Special points for Brillonin-zone integrations*, Phys. Rev. B **13**, 5188 (1976).

[66] A. Dal Corso, Pseudopotentials periodic table: From H to Pu, Comput. Mater. Sci. **95**, 337 (2014).

[67] K. Okhotnikov, T. Charpentier, and S. Cadars, Supercell program: A combinatorial structure-generation approach for the local-level modeling of atomic substitutions and partial occupancies in crystals, J. Cheminform. **8**, 1 (2016).